by pre-saturating the powder with water,[46] which is in good agreement with our own observation that pre-adsorbed water prevents benzene decomposition on Ru(001) (Figure 10). Our work indicates that the barrier for benzene dissociation—or, at least, for the irreversible formation of a molecular precursor to dissociation—on ruthenium is unusually low. This may be important for understanding reactions such as benzene hydrogenation or cyclohexane dehydrogenation, in which decomposition products can play a key role.

In summary, we find that between one-half and one-fourth of a full layer of benzene either dissociates or irreversibly forms a molecular precursor to dissociation, upon adsorption at 85 K. This has a strong influence on the coadsorbed benzene which does not dissociate, as evidenced in the thermal desorption spectra. Some benzene chemisorbs weakly (9–11 kcal/mol) at the remaining open metal sites; some forms a metastable multilayer (heat of sublimation = 7 kcal/mol) which grows under the influence of the surface layer; and some desorbs in a normal bulk multilayer (heat of sublimation = 10 kcal/mol). Desorption is complete by 180 K. Water can prevent benzene decomposition but cannot displace benzene from the dissociative phase once it has formed.

Acknowledgments. We thank S.-L. Chang and D. K. Flynn for assistance in the experiments. This research has been supported in part by a Cottrell Research Grant from the Research Corporation, and in part by the Director for Energy Research, Office of Basic Energy Sciences. Ames Laboratory is operated for the U.S. Department of Energy by Iowa State University under Contract No. W-7405-ENG-82. One of us (P.A.T.) is grateful for support of this research via a Fellowship from the Alfred P. Sloan Foundation.

Registry No. Ru, 7440-18-8; C_6H_6, 71-43-2; H_2O, 7732-18-5.

Energy Degradation Pathways and Binding Site Environment of Micelle Bound Ruthenium(II) Photosensitizers

W. J. Dressick,[†] J. Cline, III,[†] J. N. Demas,*[†] and B. A. DeGraff*[‡]

Contribution from the Chemistry Department, University of Virginia, Charlottesville, Virginia 22901, and Chemistry Department, James Madison University, Harrisonburg, Virginia 22807. *Received December 27, 1985*

Abstract: A series of α-diimine Ru(II) sensitizers were studied in aqueous, alcohol, and sodium lauryl sulfate (NaLS) micellar solutions. The emission efficiency, lifetime, and spectra change dramatically on micellization. From the temperature dependence of the excited-state lifetime and luminescence quantum efficiencies, coupled with spectral fitting, we interpret these changes and elucidate the environment of the micellized sensitizer. The increased efficiencies and lifetimes on micellization arise from decreased rates of deactivation via the photoactive d–d state and by a decrease in other intramolecular nonradiative paths. Radiationless decay theory permits semiquantitative calculation of nonradiative rate constants. A model describing the binding site and local solvent environment for the sensitizers is proposed. Implications of the results for solar energy conversion schemes are described.

We are currently studying the photochemistry and photophysics of α-diimine Ru(II) photosensitizers and their interactions in organized media. Our interest is due, in part, to the potential applicability of such systems in solar energy storage schemes.[1-6] Micelles can sequester either reactants or photoproducts and thereby retard energy wasting back reactions.[7-9]

In order to more fully understand the role of organized media in such systems, we have embarked on a systematic study of the photochemistry and photophysics of micellized sensitizers. The Ru(II) sensitizers strongly associate with anionic sodium lauryl sulfate (NaLS) as well as neutral Triton and Brij micelles.[10-16] Upon micellization, significant changes occur in the sensitizer's excited-state lifetime,[10,17-19] luminescence efficiency, and emission band shape.[14,19] These changes reflect the substantial variations in the environment of the emitting metal-to-ligand charge-transfer (MLCT) state on micellization.

We have shown that, especially for NaLS, the Ru(II) sensitizers are tightly micelle bound.[11,16,19] Using the deuterium isotope effect on excited-state lifetimes, we have estimated the degree of aqueous solvent exposure of the bound sensitizers.[16] These results, coupled with earlier $HgCl_2$ quenching results,[11] suggest that sensitizer binding occurs in the Stern layer near the surface of the NaLS micelle.

Although our results leave little doubt as to the binding region in the NaLS micelle, important questions remain concerning the details of the sensitizer's local solvent environment and to what extent it is responsible for the large spectral and lifetime effects

[†] University of Virginia.
[‡] James Madison University.

(1) Calvin, M. *Photochem. Photobiol.* **1983**, *37*, 349.
(2) Fendler, J. H. *J. Phys. Chem.* **1980**, *84*, 1485.
(3) Turro, N. J.; Grätzel, M.; Braun, A. M. *Angew. Chem., Int. Ed. Engl.* **1980**, *19*, 675.
(4) Kalyanasundaram, K. *Chem. Soc. Rev.* **1978**, *7*, 432.
(5) Grätzel, M. *Micellization, Solubilization and Microemulsions*; Mittal, K. L., Ed.; Plenum: New York, 1977; p 531.
(6) Thomas, J. K. *Modern Fluorescence Spectroscopy*; Wehry, E. L., Ed.; Plenum: New York, 1976; p 196.
(7) Takayanagi, T.; Nagamura, T.; Matsuo, T. *Ber. Bunsenges. Phys. Chem.* **1980**, *84*, 1125.
(8) Brugger, P.; Infelta, P. P.; Braun, A.; Grätzel, M. *J. Am. Chem. Soc.* **1981**, *103*, 320.
(9) Nagamura, T.; Kurihara, T.; Matsuo, T. *J. Phys. Chem.* **1982**, *86*, 1886.
(10) Mandal, K.; Hauenstein, B. L.; Demas, J. N.; DeGraff, B. A. *J. Phys. Chem.* **1983**, *87*, 328.
(11) Dressick, W. J.; Hauenstein, B. L.; Demas, J. N.; DeGraff, B. A. *Inorg. Chem.* **1984**, *23*, 1107.
(12) Dressick, W. J.; Raney, K. W.; Demas, J. N.; DeGraff, B. A. *Inorg. Chem.* **1984**, *23*, 875.
(13) Hauenstein, B. L.; Dressick, W. J.; Gilbert, T. B.; Demas, J. N.; DeGraff, B. A. *J. Phys. Chem.* **1984**, *88*, 1902.
(14) Dressick, W. J.; Demas, J. N.; DeGraff, B. A. *J. Photochem.* **1984**, *24*, 45.
(15) Dressick, W. J.; Hauenstein, B. L.; Gilbert, T. B.; Demas, J. N.; DeGraff, B. A. *J. Phys. Chem.* **1984**, *88*, 3337.
(16) Hauenstein, B. L.; Dressick, W. J.; Buell, S. L.; Demas, J. N.; DeGraff, B. A. *J. Am. Chem. Soc.* **1983**, *105*, 4251.
(17) Atherton, S. J.; Baxendale, J. H.; Hoey, B. M. *J. Chem. Soc., Faraday Trans. 1* **1982**, *78*, 2167.

0002-7863/86/1508-7567$01.50/0

Table I. Excited-State Parameters in Aqueous Solution

complex[a]	τ^b (ns)	ϕ_r^c	k^d ($s^{-1} \times 10^{-5}$)	k'^d ($s^{-1} \times 10^{-12}$)	ΔE^d (cm^{-1})	k_r^d ($s^{-1} \times 10^{-4}$)	k_{nr}^{obsd} ($s^{-1} \times 10^{-5}$)
$Ru(bpy)_3^{2+}$	580	0.042[e]	12.9	10.00	3560	6.90	12.2
$Ru(Me_2(bpy))_3^{2+}$	360	0.0286	23.6	0.122	2608	7.61	22.80
$Ru(phen)_3^{2+}$	906	0.057	3.13	9.67	3389	6.00	2.53
$Ru(Cl(phen))_3^{2+}$	946	0.068	3.44	8.20	3369	6.83	2.76
$Ru(Me(phen))_3^{2+}$	1358	0.079	3.66	14.3	3624	5.56	3.10
$Ru(4,7\text{-}Me_2(phen))_3^{2+}$	1657	0.0665	2.98	0.916	3090	3.82	2.60
$Ru(5,6\text{-}Me_2(phen))_3^{2+}$	1800	0.0656	4.15	2.15	3440	3.47	3.80
$Ru(Me_4(phen))_3^{2+}$	1648	0.0525	2.07	30.6	3762	3.03	1.77
$(phen)_2Os(DPPene)^{2+}$	1170	0.190	8.55			1.55	7.00

[a] Complexes present as Cl^- or ClO_4^- salts. [b] Excited-state lifetime in Ar bubble-degassed solution at 25.0 ± 0.2 °C. Uncertainty is 2%. [c] Radiative quantum yield in deaerated solution. Uncertainty is ±10%. T = 25.0 ± 0.2 °C. [d] Errors for the parameters are the following: k, 2%; k', 15%; ΔE, 25–50 cm^{-1}; k_r; 15%; k_{nr}^{obsd}, 4%. All parameters were measured in deaerated solution. [e] Value from ref 34.

observed. Recently, a quantitative description of the decay of the MLCT state of Os(II) and Ru(II) sensitizers using radiationless decay theory has been proposed for homogeneous media.[20-25] This study accounted, at least in part, for solvent effects on emission spectra.[25] Such methodologies should provide a powerful probe of the bound sensitizer's environment. We report here the first application of radiationless decay theory to micellar systems, specifically that of α-diimine Ru(II) complexes bound to NaLS micelles. In conjunction with the temperature dependence of the MLCT lifetimes and absolute luminescence efficiencies, our results lead to a more detailed description of the sensitizer–solvent–micelle interaction.

Experimental Section

The ligands and our abbreviations are the following: 2,2′-bipyridine (bpy), 1,10-phenanthroline (phen), 5-chloro-1,10-phenanthroline (Cl-(phen)), 5-methyl-1,10-phenanthroline (Me(phen)), 5,6-dimethyl-1,10-phenanthroline (5,6-Me_2(phen)), 4,7-dimethyl-1,10-phenanthroline (4,7-Me_2(phen)), and 3,4,7,8-tetramethyl-1,10-phenanthroline (Me_4-(phen)). Complexes were synthesized as described earlier.[26,27] Water was redistilled from alkaline $KMnO_4$. Alcohols and D_2O (Aldrich) were used as received. BioRad NaLS was recrystallized from methanol.

Sensitizer concentrations were kept to <10 μM to avoid problems with self-absorption or multiple micelle occupancy.[28] The emission spectra and absolute luminescence quantum yields (ϕ_r) were obtained in 10 mM NaLS. Because the critical micelle concentration (cmc) varies with temperature,[30] we used 50 mM NaLS in the temperature studies on excited-state lifetimes, τ, to ensure that [micelle] ≫ [Ru(II)]. At room temperature, we verified that τ's and ϕ's were identical in 10 and 50 mM NaLS. In the 298 K experiments, solutions were degassed by purging with solvent-saturated Ar (~30 min) in a thermostated cell described previously.[31]

Emission Lifetimes. Sensitizer lifetimes were obtained over the 8–50 °C range with a N_2 laser lifetime apparatus.[32] The range was limited by micelle precipitation below 8 °C and difficult temperature control and solvent evaporation at higher temperatures. Temperatures were accurate to 0.2 °C. All samples were deoxygenated.

τ's were calculated from least-squares fits to the semilogarithmic plots of intensity vs. time. Decays were exponential over at least 2 half-lives. Reported τ's are averages for at least 5 measurements (typical ±2% precision).

The temperature dependence of τ was fit to the standard model for deactivation of CT excited states.[4] This model, shown schematically in Figure 1, involves a competition between radiative decay and quenching of the emitting CT state to the ground state and deactivation via a thermally activated d–d state (vide infra). The rate equations are given by

$$1/\tau(T) = k + k_{dd} \quad (1a)$$

$$k = k_r + k_{nr} \quad (1b)$$

$$k_{dd} = k' \exp(-\Delta E/RT) \quad (1c)$$

where k is the sum of the temperature independent radiative, k_r, and radiationless, k_{nr}, rate constants for direct deactivation of the emitting state, respectively. k_{dd} is the temperature dependent radiationless decay rate constant for deactivation via a d–d excited state. Details are given later. Data were fit to eq 1 with a nonlinear least-squares simplex program.[33] Unit weights were assumed. At least 15 temperatures were used for each system.

Luminescence Spectra and Quantum Yields. Corrected emission spectra (relative quanta/cm^{-1} of bandwidth per sec) were obtained at 298 and at 77 K on an SLM Instruments 8000 spectrofluorimeter.[32] Spectra were obtained over the region 500–800 nm with a 4-nm band-pass. Spectra at 77 K were obtained in liquid N_2 with an optical Dewar flask and 1-mm-bore capillary cells. Micelle solutions were quick-frozen to preserve the solution structure.[35]

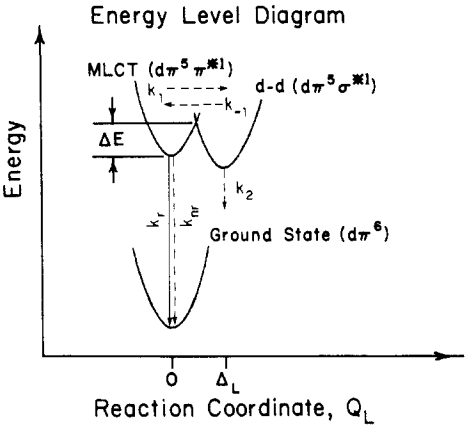

Figure 1. Energy level diagram for the RuL_3^{2+} showing paths of energy degradation. The relative state positions of the ground, MLCT, and d–d states are shown as a function of the distortion along the Ru–N bond, Q_L. ΔE is the barrier height for the MLCT → d–d transition.

(18) Baxendale, J. H.; Rodgers, M. A. J. *J. Phys. Chem.* **1982**, *86*, 4906.
(19) (a) Buell, S. L. Ph.D. Dissertation, University of Virginia, 1983. (b) Snyder, S. M.S. Thesis, University of Virginia, 1985.
(20) Caspar, J. V.; Kober, E. M.; Sullivan, B. P.; Meyer, T. J. *J. Am. Chem. Soc.* **1982**, *104*, 630.
(21) Caspar, J. V.; Sullivan, B. P.; Kober, E. M.; Meyer, T. J. *Chem. Phys. Lett.* **1982**, *91*, 91.
(22) Caspar, J. V.; Meyer, T. J. *J. Phys. Chem.* **1983**, *87*, 952.
(23) Caspar, J. V.; Meyer, T. J. *J. Am. Chem. Soc.* **1983**, *105*, 5583.
(24) Caspar, J. V.; Meyer, T. J. *Inorg. Chem.* **1983**, *22*, 2444.
(25) Caspar, J. V. Ph.D. Dissertation, The University of North Carolina, Chapel Hill, 1982.
(26) Braddock, J. N.; Meyer, T. J. *J. Am. Chem. Soc.* **1973**, *95*, 3158.
(27) Demas, J. N.; Turner, T. F.; Crosby, G. A. *Inorg. Chem.* **1969**, *8*, 674.
(28) The micelle concentration is calculated from [M] = ([S] − cmc)/N where [M] = micelle concentration, [S] = total surfactant concentration, cmc = critical micelle concentration, and N = aggregation number. For NaLS, cmc < 8.1 mM and N = 62[29] so 10 mM NaLS corresponds to >3.2 × 10^{-5} M micelles. Micelle occupancy is governed by Poisson statistics for our systems.[3] Occupancy of the micelle by not more than one sensitizer is insured if [M] > [sensitizer].
(29) Fendler, J. H.; Fendler, E. J. *Catalysis in Micellar and Macromolecular Systems*; Academic: New York, 1975; p 21.
(30) Mukerjee, P.; Mysels, K. J. *Critical Micelle Concentrations of Aqueous Surfactant Systems*, U.S. Department of Commerce, National Bureau of Standards: Washington, DC, 1970; NRSDS-NBS 36.
(31) (a) Buell, S.; Demas, J. N. *Anal. Chem.* **1982**, *54*, 1214. (b) Buell, S.; Demas, J. N. *Rev. Sci. Instrum.* **1982**, *53*, 1298.
(32) (a) Turley, T. J. M.S. Thesis, University of Virginia, 1980. (b) Turley, T. J.; Demas, J. N.; Demas, D. J., submitted.
(33) (a) Daniels, R. W. *An Introduction to Numerical Methods and Optimization Techniques*; North Holland: New York, 1978. (b) Demas, J. N. *Excited State Lifetime Measurements*; Academic: New York, 1983. (c) Bevington, P. R. *Data Reduction and Error Analysis for the Physical Sciences*; McGraw-Hill: New York, 1969.
(34) Parker, C. A.; Rees, W. T. *Analyst* **1960**, *85*, 587.

Table II. Excited-State Parameters in 50 mM NaLS Solutions

complex[a]	τ^b (ns)	ϕ_r^c	k^d ($s^{-1} \times 10^{-5}$)	k'^d ($s^{-1} \times 10^{-12}$)	ΔE^d (cm^{-1})	k_r^d ($s^{-1} \times 10^{-4}$)	k_{nr}^{obsd} ($s^{-1} \times 10^{-5}$)
$Ru(bpy)_3^{2+}$	800	0.055	10.68	2.15	3374	6.52	10.0
$Ru(Me_2(bpy))_3^{2+}$	614	0.038	14.1	0.0041	2039	5.90	13.5
$Ru(phen)_3^{2+}$	1818	0.104	2.24	215.0	4223	5.48	1.69
$Ru(Cl(phen))_3^{2+}$	2140	0.124	2.20	73.8	4044	5.53	1.65
$Ru(Me(phen))_3^{2+}$	2367	0.141	2.44	102.0	4180	5.67	1.87
$Ru(4,7\text{-}Me_2(phen))_3^{2+}$	3412	0.144	1.70	20.8	3933	4.01	1.30
$Ru(5,6\text{-}Me_2(phen))_3^{2+}$	2990	0.093	2.39	13.4	3909	2.96	2.09
$Ru(Me_4(phen))_3^{2+}$	2197	0.067	1.10	19.8	3706	2.90	0.81

[a] Complexes present as Cl^- or ClO_4^- salts. [b] Excited-state lifetimes in deaerated solution at 25.0 ± 0.2 °C. Uncertainty is 2%. [c] Radiative quantum yield in deaerated solution. Uncertainty is 10%. T = 25.0 ± 0.2 °C. [d] Errors for the parameters are the following: k, 2%; k', 15%; ΔE, 25–50 cm^{-1}; k_r 15%; k_{nr}, 4%. All parameters were measured in deaerated solution.

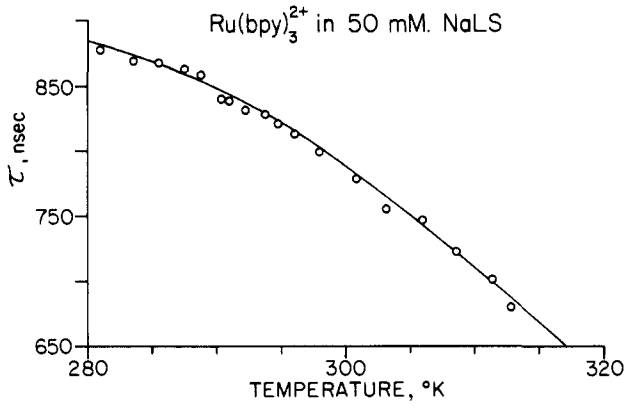

Figure 2. Temperature dependence of the $Ru(bpy)_3^{2+}$ lifetime in a deoxygenated 50 mM NaLS solution: (O) experimental data; (—) best fit with eq 1.

Absolute luminescence quantum yields, ϕ_r, were measured by a Parker–Rees method[34] relative to an aqueous $Ru(bpy)_3^{2+}$ standard (ϕ_r = 0.042).[36] All solutions were deaerated (T = 25.0 ± 0.5 °C). Refractive index corrections were ignored since water and 10 mM NaLS have the same refractive index. k_r's and k_{nr}'s were determined from the τ's and ϕ_r's with

$$k_r = \phi_r \tau^{-1} \phi_{isc}^{-1} \quad (2)$$

$$k_{nr} = k - \phi_r \tau^{-1} \phi_{isc}^{-1} \quad (3)$$

where the intersystem crossing efficiency, ϕ_{isc}, was taken as unity.

Spectral Fitting. Digitized luminescence spectra (150 points) were fit to eq 4 (vide infra) with a nonlinear least-squares Marquardt program.[33] Best fit parameters and statistical uncertainties were calculated by assuming unit weights. Vibrational frequencies in all fittings were fixed at ω_L = 1350 cm^{-1} and ω_M = 400 cm^{-1}. ω_L and ω_M are compromise values and probably have a spread of at least 50 cm^{-1}.

Results

Figure 2 shows a representative temperature dependence of τ and the fit to eq 1 ($Ru(bpy)_3^{2+}$ in 50 mM NaLS). At lower temperatures, τ asymptotically approaches a limiting value, while at higher temperatures τ decreases rapidly with increasing temperature. Tables I and II list the parameters obtained by fitting data with use of eq 1 for both aqueous and micellar solutions. Values of k, k', ΔE, τ, ϕ_r, k_r, and k_{nr} are listed.

Fitting to eq 1 provides a measure of micellar properties only if the sensitizer is tightly bound over the temperature range examined. While at room temperature, the α-diimine Ru(II) complexes are strongly bound to the NaLS micelle;[11,19,37] changes in binding with temperature could produce errors. k, k', and ΔE would then be averaged over the bound and unbound sensitizer forms.

We show that sensitizer binding is tight over our temperature range by measuring the apparent solvent exposure of the sensitizer at several temperatures. The H_2O exposures are 0.27 ± 0.06, 0.30 ± 0.05, and 0.29 ± 0.07 at 42, 25, and 15 °C, respectively, for $Ru(bpy)_3^{2+}$ in 50 mM NaLS solution.[16] The invariance of solvent exposure shows that the complex remains completely micellized over our temperature range, and there are no radical changes in the sensitizer's environment. Thus, k, k', and ΔE are valid measurements for NaLS micelle-bound sensitizers. We infer similar behavior for the remaining complexes.

Emission spectra were fit to the theoretical equation

$$I(E) = \sum_{n=0}^{5}\sum_{m=0}^{5} I_{nm}(E) = \sum_{n=0}^{5}\sum_{m=0}^{5} (\{E^{OO} - n\hbar\omega_M - m\hbar\omega_L\}/E^{OO})^4 (S_M{}^n/n!) \times (S_L{}^m/m!) \exp[(-4 \ln 2)(\{E - E^{OO} + n\hbar\omega_M + m\hbar\omega_L\}/\nu_{1/2})^2] \quad (4)$$

Equation 4 was derived with the assumption that excited-state deactivation occurs primarily along two normal coordinates characterized by frequencies ω_M and ω_L.[25,38,39] Our notation conforms to that used earlier. One vibration involves α-diimine ring deformations and is characterized by ω_M = 1350 cm^{-1}. A second deactivation mode has $\omega_L \cong$ 400 cm^{-1} and corresponds to a normal coordinate primarily comprised of a Ru–N stretch. The derivation of eq 4 and the assignment of ω_M and ω_L for the Ru(II) sensitizers are given elsewhere.[20-25] The prior justification for terminating the summations at 5[25] applies here.

The remaining factors in eq 4 are as follows: (1) $I(E)$ is the normalized emission intensity at energy E (cm^{-1}); (2) $I_{nm}(E)$ is the contribution to $I(E)$ from a single vibronic component (emission is assumed to arise from the lowest MLCT vibrational state to the state comprised of the nth vibrational level of ω_M and the mth level of ω_L in the ground state); (3) E^{OO} is the energy of the 0–0 MLCT electronic transition (cm^{-1}); (4) $\nu_{1/2}$ is the full-width at half-maximum (cm^{-1}) for the vibronic components, $I_{nm}(E)$; and (5) S_i is the phonon-coupling strength (Huang–Rhys factor) for the normal coordinate of ω_i. The factor is defined by

$$S_i = \Delta^2{}_i/2 = 1/2(Q_i^g - Q_i^e)^2(\mu_i\omega_i)/\hbar \quad (5)$$

where Q_i^g and Q_i^e are the equilibrium positions of the ground and excited states along the ith normal coordinate and μ_i is the reduced mass of the ith vibration. Δ is a mass weighted dimensionless shift in the equilibrium positions of the ground and excited states. The S_i's describe the distortion from the ground-state equilibrium position that occurs along normal coordinate ω_i upon excitation. An S of zero signifies that there is no molecular distortion along the corresponding normal coordinate. S_L and S_M represent the distortions occurring along the ω_L and ω_M acceptor vibrations, respectively.

(35) Narayana, P. A.; Li, A. S. W.; Kevan, L. *J. Phys. Chem.* **1982**, *86*, 3.
(36) Van Houten, J.; Watts, R. J. *J. Am. Chem. Soc.* **1976**, *98*, 4853.
(37) Meisel, D.; Matheson, M. S.; Rabani, J. *J. Am. Chem. Soc.* **1978**, *100*, 117.

(38) A 2-mode fit must at best be an approximation to such large vibration rich complexes. For example, there are 7 modes in the 1000–1600-cm^{-1} region.[39] However, under most conditions a group of similar frequency modes can be treated as a single mode. The vibrational frequency then becomes a weighted average of the contributions, and S is the sum of all the S_i's contributing to the average mode.[39] In the current work this approximation has no effect on our conclusions.
(39) Kober, E. M.; Meyer, T. J. *Inorg. Chem.* **1985**, *24*, 106.

Table III. Emission Parameters in Aqueous Solution[a]

complex	E^{00} (cm^{-1})[b]	S_M	S_L	$\nu_{1/2}$ (cm^{-1})
$Ru(bpy)_3^{2+}$	17006 ± 132	1.145 ± 0.021	2.074 ± 0.39	1391 ± 41
$Ru(Me_2(bpy))_3^{2+}$	16645 ± 188	1.007 ± 0.030	2.606 ± 0.56	1649 ± 62
$Ru(phen)_3^{2+}$	17032 ± 164	1.044 ± 0.026	0.742 ± 0.26	1602 ± 50
$Ru(Cl(phen))_3^{2+}$	16990 ± 104	1.064 ± 0.010	0.644 ± 0.22	1566 ± 40
$Ru(Me(phen))_3^{2+}$	16901 ± 110	1.044 ± 0.024	0.697 ± 0.20	1599 ± 43
$Ru(4,7\text{-}Me_2(phen))_3^{2+}$	17101 ± 149	1.026 ± 0.031	1.907 ± 0.40	1526 ± 45
$Ru(5,6\text{-}Me_2(phen))_3^{2+}$	17065 ± 162	0.966 ± 0.018	1.779 ± 0.48	1472 ± 58
$Ru(Me_4(phen))_3^{2+}$	17261 ± 150	1.065 ± 0.020	1.930 ± 0.41	1541 ± 51

[a] At 25.0 ± 0.5 °C in deaerated solution. [b] Parameters calculated from emission spectra with eq 4.

Table IV. Emission Parameters in 10 mM NaLS Solution[a]

complex	E^{00} (cm^{-1})[b]	S_M	S_L	$\nu_{1/2}$ (cm^{-1})
$Ru(bpy)_3^{2+}$	15991 ± 74	1.034 ± 0.015	0.625 ± 0.193	1477.1 ± 26.0
$Ru(Me_2(bpy))_3^{2+}$	15521 ± 53	1.076 ± 0.036	0.000 ± 0.249	1529.1 ± 26.2
$Ru(phen)_3^{2+}$	16424 ± 46	0.992 ± 0.011	0.081 ± 0.012	1421.2 ± 33.5
$Ru(Cl(phen))_3^{2+}$	16332 ± 38	0.958 ± 0.034	0.246 ± 0.140	1429.5 ± 35.9
$Ru(Me(phen))_3^{2+}$	16461 ± 53	0.965 ± 0.013	0.271 ± 0.300	1380.5 ± 38.0
$Ru(4,7\text{-}Me_2(phen))_3^{2+}$	16271 ± 42	1.029 ± 0.011	0.032 ± 0.110	1471.2 ± 30.1
$Ru(5,6\text{-}Me_2(phen))_3^{2+}$	16412 ± 45	0.971 ± 0.014	0.170 ± 0.223	1401.5 ± 27.2
$Ru(Me_4(phen))_3^{2+}$	16553 ± 49	1.062 ± 0.015	0.100 ± 0.163	1465.1 ± 25.5

[a] At 25.0 ± 0.5 °C in deaerated solution. [b] Parameters calculated from emission spectra with eq 4.

Table V. Emission Parameters for $Ru(4,7\text{-}Me_2(phen))_3^{2+}$ in Hydroxylic Solvents

solvent	T^a	E^{00} (cm^{-1})[b]	S_M	S_L	$\nu_{1/2}$ (cm^{-1})
H_2O	298	17101 ± 149	1.026 ± 0.031	1.907 ± 0.402	1526 ± 45
methyl alcohol	298	16859 ± 94	1.157 ± 0.010	0.00	1589 ± 39
ethyl alcohol	298	16860 ± 92	1.116 ± 0.012	0.00	1583 ± 42
n-butyl alcohol	298	16884 ± 87	1.137 ± 0.012	0.00	1611 ± 44
n-hexyl alcohol	298	16710 ± 96	1.125 ± 0.014	0.00	1632 ± 43
n-hexyl alcohol	77	17728 ± 112	1.008 ± 0.009	1.419 ± 0.311	609 ± 49
n-octyl alcohol	298	16649 ± 91	1.100 ± 0.010	0.00	1652 ± 48
n-decyl alcohol	298	16618 ± 83	1.095 ± 0.009	0.00	1660 ± 60
n-decyl alcohol	77	17785 ± 102	1.063 ± 0.009	1.768 ± 0.336	614 ± 51
50 mM NaLS	298	16271 ± 42	1.029 ± 0.011	0.032 ± 0.110	1471 ± 30
50 mM NaLS	77	17496 ± 98	0.934 ± 0.024	1.012 ± 0.404	719 ± 58

[a] In K. Uncertainty is ~0.5 K. [b] Parameters calculated from emission spectra with eq 4.

Table VI. k_{nr} Ratios

complex	$k_{nr}^{NaLS}/k_{nr}^{H_2O}$[a] (spectral study)	$k_{nr}^{NaLS}/k_{nr}^{H_2O}$[b] (lifetime study)	f_{OH}[c]
$Ru(bpy)_3^{2+}$	0.79 ± 0.28	0.82 ± 0.06	0.305 ± 0.047
$Ru(Me_2(bpy))_3^{2+}$	0.97 ± 0.34	0.59 ± 0.05	0.246 ± 0.036
$Ru(phen)_3^{2+}$	0.90 ± 0.33	0.67 ± 0.05	0.357 ± 0.049
$Ru(Cl(phen))_3^{2+}$	0.72 ± 0.25	0.60 ± 0.05	0.438 ± 0.017
$Ru(Me(phen))_3^{2+}$	0.58 ± 0.21	0.60 ± 0.05	0.156 ± 0.085
$Ru(4,7\text{-}Me_2\text{-}(phen))_3^{2+}$	1.09 ± 0.40	0.50 ± 0.04	0.246 ± 0.007
$Ru(5,6\text{-}Me_2\text{-}(phen))_3^{2+}$	0.98 ± 0.34	0.55 ± 0.04	0.287 ± 0.051
$Ru(Me_4(phen))_3^{2+}$	0.84 ± 0.30	0.46 ± 0.04	0.373 ± 0.222

[a] Calculated from the data in Tables III and IV. [b] Calculated from the data in Tables I and II. [c] Solvent H_2O exposure parameters from ref 16.

Figure 3 shows the fit of the $Ru(5,6\text{-}Me_2(phen))_3^{2+}$ emission (10 mM NaLS) to eq 4. The high equality fit is typical. The least-squares parameters are summarized in Table III (pure water) and Table IV (10 mM NaLS). Tables I, III, and IV show that E^{00} and S_L change appreciably upon micellization while S_M and $\nu_{1/2}$ are much less affected. Parameters were insensitive to the initial guesses.

Table V shows the behavior of a typical sensitizer, $Ru(4,7\text{-}Me_2(phen))_3^{2+}$, in various alcohols and for micellar solutions (77 and 298 K). E^{00} and S_L for the alcohols and the micellar solution are similar. For the alcohols, the S_M's are slightly higher than for the micelles, but the $\nu_{1/2}$'s are much greater.

Table VI compares the ratio of k_{nr}'s in water to NaLS with spectral fitting (eq 4 and 6) to that determined from the temperature dependence of τ (Tables I and II). For perfect agreement between the two approaches, the ratios should be equal. Also shown is the degree of water exposure, f_{OH}, for the bound sensitizers.[16] The ratios given by the two methods diverge with decreasing f_{OH}.

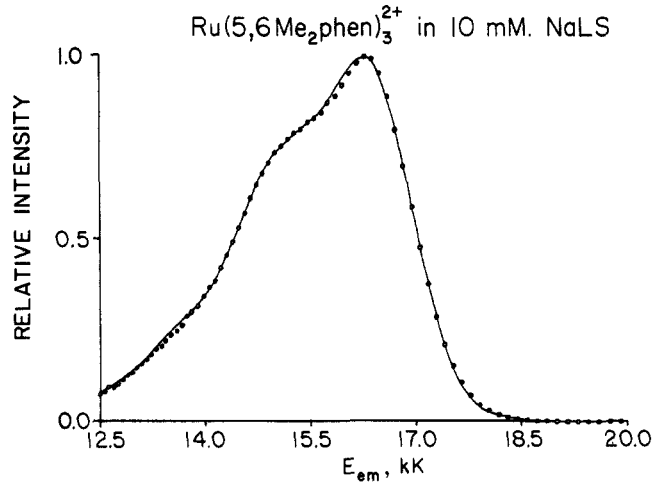

Figure 3. Emission spectrum of $Ru(5,6\text{-}Me_2(phen))_3^{2+}$ in 10 mM NaLS solution. The circles are the experimental data and the solid line represents the least squares fit to the data with eq 4. For clarity, only half of the experimental points are shown. The spectrum is normalized to unity at the emission maximum. The experimental conditions are λ_{ex} = 450 nm, T = 298 K, Ar degassed solution.

Discussion Section

Interactions of α-diimine Ru(II) complexes with surfactants can yield significant, and potentially useful, changes in sensitizer properties. Changes occur in redox potentials,[40-42] excited-state

lifetimes,[10,11,19] emission spectra, and vibrational structure.[14,19] For example, addition of NaLS at concentrations above the cmc to aqueous $Ru(bpy)_3^{2+}$ sharpens the emission, shifts the emission from orange to red, and increases the emission lifetime from 580 to 800 ns. Any model of micellized sensitizers should rationalize these changes.

We first summarize the salient properties of the MLCT excited state of Ru(II) complexes in a variety of homogeneous media including water[24,43,44] and aprotic organic solvents.[25,43,45-48] The following information is available:

(1) For $Ru(bpy)_3^{2+}$, MLCT emission occurs from a manifold of three closely spaced ($\sim$100 cm^{-1}) states.[22,23,25,49-51] At high temperatures (>200 K), all states are thermally populated and contribute to the excited-state decay. At room temperature the emitting manifold has substantial singlet and triplet character, although the emitting state is routinely referred to as a "triplet".[52]

(2) In fluid media, the MLCT state is best described as a Ru(III) center with a localized single reduced α-diimine ligand (radical anion), rather than as a state delocalized over multiple ligands.[53-57] This localization appears to arise from molecular distortion in the excited state that lowers the energy of one of the ligand localized states and tends to trap the electron. The charge-transfer character of the excited state provides a basis for the solvent effects on the sensitizer properties.[17-19,43,23,25,58]

(3) In rigid media, where molecular motions cannot occur rapidly, molecular distortions cannot produce a localized electron trap.[56,57] Under these conditions the excited states are best described as delocalized.

(4) Absorption initially populates an MLCT state, which is largely singlet in character. Intersystem crossing to the "triplet" emitting states occurs with unit efficiency ($\phi_{isc} = 1$) in MeOH and H_2O at room temperature.[59] Other work suggests solvent independence of ϕ_{isc}.[23,25]

(5) Deactivation of the emitting state at high temperatures can occur directly to the ground state or through a nonemissive d–d state (Figure 1). Direct decay to the ground state can occur via both radiative and nonradiative paths with first-order rate constants k_r and k_{nr}, respectively. Thermal crossing to a d–d excited state, $^*CT \rightarrow {}^*d\text{–}d$, represents a second nonradiative pathway.[23,25]

We point out a major difference in the properties of an excited state in a microheterogeneous environment vs. a homogeneous one. The microheterogeneous NaLS environment enhances the inequivalency of the ligands and leads to a deeper trap for the electron on the radical anion. From an electrostatic standpoint, the most reasonable ligand for electron localization is the one that projects into the aqueous solvent. The electron would then be relatively free to move away from the anionic sulfate groups, especially when accompanied by molecular distortion. An excited state in such an assymmetric environment would be quite different from one in a homogeneous environment, and we would expect any homogeneous model for such an excited state to provide, at best, only a partial description of the spectral properties. We realize that this simple picture will be complicated by micellar and sensitizer dynamics as well as by the possibility of electron migration between rings, but we believe that the basic picture is sound.

Deactivation Pathways. The model of Figure 1 leads to eq 1, which relates the observed emission lifetime to k_r, k_{nr}, and k_{dd}. Values of k', ΔE, k_r, and k_{nr} are obtained from measured quantities with eq 1–4. These parameters provide the key to understanding the effects of micellization on paths of excited-state energy degradation. Since the τ's increase on micellization, k_r, k_{nr}, and/or k_{dd} are affected. The relative importance of each is shown in Tables I and II. Within experimental error, k_r is invariant (<9%) on micellization; this is consistent with the insensitivity of k_r for $Ru(bpy)_3^{2+}$ in different aprotic solvents.[23,25] Thus, the changes in τ arise from changing radiationless rates. Relaxation to the ground state via the d–d state is also markedly affected by micellization, and the k_{dd}'s are reduced by $\sim$50%.

k_{nr} is governed, at least in part, by the energy gap law.[20-25,43] This theory allows us to correlate k_{nr} with emission spectra. k_{nr} is given by

$$\ln k_{nr} = \ln \beta_o - S_M - (\gamma_o E^{OO}/\hbar\omega_M) + (\chi_o/\hbar\omega_M) \times (k_B T/\hbar\omega_M)(\gamma_o + 1)^2 + S_L(\omega_L/\omega_M)(\gamma_o + 1) \quad (6)$$

$$\beta_o = |C^k|^2\omega_k \left[\frac{\pi}{2\hbar\omega_M(E^{OO} - \hbar\omega_L S_L)} \right]^{1/2} \quad (7)$$

$$\gamma_o = \ln [E^{OO}/\hbar\omega_M S_M] - 1 \quad (8)$$

$$\chi_o = (\nu_{1/2})^2/(16 k_B T \ln 2) \quad (9)$$

where k_B is the Boltzmann constant, T is the absolute temperature (K), and χ_o (cm^{-1}) is the classical outer-sphere reorganization energy for the decay process. $|C^k|$ is the nuclear momentum matrix element and ω_k the promoting mode frequency for the transition. The remaining parameters are described elsewhere,[20-25] and we obtain them from multiparameter emission fits (eq 4).

Equation 6 characterizes k_{nr} as occurring through one high frequency acceptor mode, one low frequency acceptor mode, and the solvent vibrations. Each term may vary with solvent since E^{OO} and the S's can depend on solvent. Also, slight decreases in $\nu_{1/2}$ (and χ_o) are observed. We model the changes on micellization by treating them as solvent effects and applying eq 6.

Earlier treatments have been able to make the simplifying assumptions that all terms except E^{OO} were constant with solvent variation. Such assumptions lead to the prediction that ln k_{nr} decreases linearly with increasing E^{OO}, as has been observed. Clearly, this is not the case here. Micellization decreases both E^{OO} and k_{nr}. This apparent violation of the energy gap law is, however, easily reconciled when we recognize that factors other than E^{OO} change on micellization. In particular, S_L is substantial in water but essentially zero on micellization.

Including the observed changes, eq 6 correctly predicts a reduction of k_{nr} on micellization. Unfortunately, we cannot calculate absolute k_{nr}'s because the $|C^k|^2\omega_k$'s are unknown. We can quantitatively test eq 6, however, by recognizing that the $|C^k|^2\omega_k$'s can be eliminated by comparing the k_{nr} terms in NaLS and aqueous solutions. The ratios $k_{nr}^{NaLS}/k_{nr}^{water}$, calculated with eq 6, are summarized in Table VI; the large uncertainties reflect mainly the large S_L errors. Also shown are the ratios determined from the observed k_{nr}'s (Tables I and II). There is a remarkably good agreement between the ratios determined by spectral (eq 6) and lifetime measurements, although there is a suggestion that the deviations increase with hydrophobicity of the complexes.

There is a fundamental reason why ratios calculated by eq 6 might be in error for micellar systems. Solvent exposure studies[16] clearly show that micellization replaces much of the water surrounding the sensitizer by aprotic LS^-. Earlier work has shown that water and typical polar organic solvents exhibit significant

(40) Ohsawa, Y.; Aoyagui, S. *J. Electroanal. Chem.* **1982**, *136*, 353.
(41) Shinozuka, N.; Hayano, S. *Solution Chemistry of Surfactants*; Mittal, K. L., Ed.; Plenum: New York, 1979; Vol. 2, p 599.
(42) Ohsawa, Y.; Shimazaki, Y.; Aoyagui, S. *J. Electroanal. Chem.* **1980**, *114*, 235.
(43) Caspar, J. V.; Meyer, T. J. *J. Am. Chem. Soc.* **1983**, *105*, 5583.
(44) Vining, W. J.; Caspar, J. V.; Meyer, T. J. *J. Phys. Chem.* **1985**, *89*, 1095.
(45) Van Houten, J.; Watts, R. J. *Inorg. Chem.* **1978**, *100*, 3381.
(46) Hoggard, P. E.; Porter, G. B. *J. Am. Chem. Soc.* **1978**, *100*, 1457.
(47) Wallance, W. M.; Hoggard, P. E. *Inorg. Chem.* **1979**, *18*, 1934.
(48) Gleria, M.; Minto, F.; Beggiato, G.; Bortolus, P. *J. Chem. Soc., Chem. Commun.* **1978**, 285.
(49) Hager, G. D.; Crosby, G. A. *J. Am. Chem. Soc.* **1975**, *97*, 7031.
(50) Kober, E. M.; Meyer, T. J. *Inorg. Chem.* **1982**, *21*, 3978.
(51) Kober, E. M. Ph.D. Dissertation, The University of North Carolina, Chapel Hill, 1982.
(52) (a) Mandal, K.; Demas, J. N. *Chem. Phys. Lett.* **1981**, *84*, 410. (b) Mandal, K.; Demas, J. N. *J. Am. Chem. Soc.* **1983**, *105*, 701.
(53) Bradley, P. G.; Kress, N.; Hornberger, B. A.; Dallinger, R. F.; Woodruff, W. H. *J. Am. Chem. Soc.* **1981**, *103*, 7441.
(54) Strukl, J. S.; Walter, J. L. *Spectrochim. Acta, Part A* **1971**, *27A*, 209.
(55) Strukl, J. S.; Walter, J. L. *Spectrochim. Acta, Part A* **1971**, *27A*, 223.
(56) Ferguson, J.; Krausz, E. R.; Maeder, M. *J. Phys. Chem.* **1985**, *89*, 1852.
(57) Krausz, E. *Chem. Phys. Lett.* **1985**, *116*, 501.
(58) Nakamura, K. *Bull. Chem. Soc. Jpn.* **1982**, *55*, 1639.
(59) Demas, J. N.; Taylor, D. G. *Inorg. Chem.* **1979**, *18*, 3177.

differences in their ability to deactivate excited states.[21,25,60] It was suggested that these differences arise from high-frequency hydrogen-bonding solvent modes, which have not been included in eq 4 and 6 or χ_o.[21,25,61] Our deuterium isotope studies[16] also show that high-frequency OH vibrations contribute a particularly effective coupling pathway for decay that is absent in aprotic solvents. The neglect of these high-frequency vibrations could account for failure of eq 6 when applied to micellized systems.

To explicitly account for such high-frequency mode(s), a term of the form $S_H(\omega_H/\omega_M)(\gamma_o + 1)$ would have to be included in eq 6. S_H represents the excited-state distortion due to solvent mode(s) of frequency ω_H ($\hbar\omega_H > k_BT$). In the absence of adequately resolved vibrational emission structure and a lack of knowledge concerning the specific value(s) of ω_H, quantitative analysis is not yet warranted. However, the addition of a high-frequency solvent term that vanishes as the solvent exposure approaches zero provides a qualitatively suitable "correction" to eq 6.

The remaining factor controlling τ is deactivation via the d–d state, k_{dd}, which is strongly influenced by micellization. For example, with $Ru(bpy)_3^{2+}$, k_{dd} decreases by ~60% on micellization while k_{nr} decreases by ~15%. In water, k_{dd} accounts for ~23% of the excited-state decay but falls to <13% on micellization.

We turn now to the question of how k_{dd} depends on fundamental processes. The model for excited-state decay including the d–d excited state is[23,25]

$$\text{MLCT} \underset{k_{-1}}{\overset{k_1}{\rightleftharpoons}} \text{d–d} \xrightarrow{k_2} \text{ground state or photochemistry}$$

There are two limiting cases. For case I $k_2 \gg k_{-1}$, and observed values of k' and ΔE have been in the ranges 10^{12}–10^{14} s^{-1} and >3000 cm^{-1}, respectively. For case II, $k_{-1} \gg k_2$, and the MLCT and d–d states are in a pseudoequilibrium. For case II systems, $k' \sim 10^{9-10}$ s^{-1} and $\Delta E \cong 2000$ cm^{-1}.

Most of the Ru(II) complexes exhibit case I behavior in both aqueous and micellar solutions. The possible exception in this work is $Ru(Me_2(bpy))_3^{2+}$. In water, k' suggests case I whereas ΔE appears somewhat too low, while in NaLS both k' and ΔE appear typical of case II. However, the above limits are only suggested and are based on rather limited data. In terms of room and low temperature emission properties, $Ru(Me_2(bpy))_3^{2+}$ appears indistinguishable from all the other complexes. In the absence of more definitive evidence we assume that all systems are case I, although there are questions concerning $Ru(Me_2(bpy))_3^{2+}$.

Typically, k_{dd} decreases on micellization. Even though k' usually increases, ΔE also increases and the exponential ΔE term dominates. As shown in Figure 1, an increase in ΔE suggests a stabilization of the MLCT state relative to the d–d state.[25] Since population of the d–d state can lead to photodegradation, Ru(II) complexes should be photostabilized on micellization. This observation is especially significant given the current interest in organized media based on solar energy conversion schemes.[3,7–9]

Binding Region. Knowledge of the binding region is critical to understanding micelle-sensitizer interactions and in developing practical applications. We utilize our results to probe differences between the aqueous and micellar environments.

In all cases, the MLCT state is stabilized on micellization relative to the ground state as reflected by decreased E^{OO}'s. Further, the CT state appears to be stabilized more with respect to the ground state than the d–d state; ΔE typically increases on micellization. Such behavior is consistent with the greater sensitivity of CT states to solvent effects relative to metal localized d–d states. E^{OO} decreases by ~600 cm^{-1} for the phen and ~1000 cm^{-1} for the bpy complexes. Also, except for $Ru(bpy)_3^{2+}$, χ_o decreases slightly upon micellization.

S_L, but not S_M, appears to be affected by micellization. This might imply that for S_L the large excited-state distortions in water seem to be completely eliminated on micellization. The exception once again is $Ru(bpy)_3^{2+}$, although S_L decreases significantly on micellization.

Before discussing our findings further, we review several properties of NaLS micellized α-diimine Ru(II) complexes:

(1) Dynamic quenching of the MLCT emission of the micelle-bound Ru(II) sensitizer by solvent-borne $HgCl_2$ occurs via electron-transfer. The quenching conforms to Marcus theory.[11]

(2) About one-third of the sensitizer is exposed to water on micellization. The exposed fraction decreases as the hydrophobicity of the sensitizer increases.[15,16]

(3) The sensitizer and LS^- form tight ion-pairs.[17–19,37]

These facts coupled with our current data provide the basis for a description of the NaLS micellized sensitizers. The important questions are the following: What is the location of the sensitizer within the micelle and what is the local solvent environment?

With regard to sensitizer location, our observations are most consistent with the binding in the Stern layer near the micelle surface. Several lines of evidence support this contention. The wet binding environment coupled with the quenching by molecules in the bulk solvent are indicative of Stern layer binding.

We can exclude two alternative interpretations. While water that penetrates the micellar interior[62–65] either in pockets or deep channels or fjords[63] could account for the wet environment of deeply embedded sensitizers, this is completely inconsistent with efficient quenching behavior. Water borne quenchers are unlikely to readily penetrate narrow fjords or to reach interior pockets.[16]

Surface sensitizer binding is also consistent with the strong ion pairing of the Ru(II) sensitizer with LS^-.[19,37] Placement of the Ru(II) sensitizer in the Stern layer satisfies the requirement for a close complex–LS^- interaction, yet positions the $RuL_3(LS)_2$ (L = α-diimine ligand) in a minimum energy position. The hydrocarbon chains of the "bound" LS^- group can interact with the micelle's hydrocarbon core. The bulky, charged sensitizer is accessible to bulk water, yet it is positioned to minimally disturb the micelle structure.

The bound sensitizer's local solvent environment is also of interest. Solvation changes on micellization are responsible, at least in part, for the successful applications of micelles in catalysis[29,66–69] and in solar energy conversion.[3,7–9]

The spectral fitting parameters are consistent with the mixed solvent nature of the Stern layer and provide additional insight into the solvent structure at the sensitizer. In the ground state, the dipositive Ru(II) complexes have no permanent dipole moment. Solvation in the Stern layer is dominated by the strong electrostatic interactions between the Ru(II) and the LS^- head groups. Interactions of the bound complex with H_2O and other LS^- groups in the Stern layer also occur.

Our emission spectra supply evidence for these interactions. The time scale for absorption is too fast for solvent reorganization to affect it. Consequently, the initially excited MLCT state sees the same environment as the ground-state conformation of the complex. At room temperature, excited-state equilibration via vibrational relaxation and solvent reorganization rapidly occurs. Emission ultimately then arises from this lower energy, thermally equilibrated (thexi) MLCT state.

In a frozen solution, however, solvent relaxation and orientation equilibration cannot occur during the excited-state lifetime since molecular motions are hindered. Emission occurs from a solvent environment representative of the ground state. For aqueous NaLS solutions, EPR experiments have shown that the micelle structure is retained on freezing.[35] Thus, the 77 K emission spectra provide a valid probe of the average ground-state solvent environment of the micellized complexes.

(60) Lin, S. H. *J. Chem. Phys.* **1966**, *44*, 3759.
(61) Guarr, T.; Buhks, E.; McLendon, G. *J. Am. Chem. Soc.* **1983**, *105*, 3763.
(62) Narayana, P.; Li, A. S.; Kevan, L. *J. Am. Chem. Soc.* **1982**, *104*, 6502.
(63) Menger, F. M. *Acc. Chem. Res.* **1979**, *12*, 111.
(64) Bendedouch, D.; Chen, S.-H.; Koehler, N. C. *J. Phys. Chem.* **1983**, *87*, 153.
(65) Menger, F. M.; Chow, J. G. *J. Am. Chem. Soc.* **1983**, *105*, 5501.
(66) Fendler, J. H. *Acc. Chem. Res.* **1980**, *13*, 7.
(67) Fendler, J. H.; Hinze, W. *J. Am. Chem. Soc.* **1981**, *103*, 5439.
(68) Stigter, D. *J. Colloid. Interfac. Sci.* **1967**, *23*, 379.
(69) Frahm, J.; Diekmann, S. *J. Colloid Interface Sci.* **1979**, *70*, 440.

Table V shows a summary of the spectral parameters for Ru(4,7-Me_2(phen))$_3^{2+}$ in NaLS micelle at 77 and 298 K. The expected E^{00} shift and changes in $\nu_{1/2}$[2,5] are observed. Of special interest are S_L and S_M, which are sensitive to the Ru–N and α-diimine ligand frame vibrations, respectively. S_L's in the frozen micelle solutions are $\sim$1 while the pure H_2O values are significantly greater (1.5–2.0).

On the basis of the preceding discussion, we present the following simple picture of micellized Ru(II) complexes. The complex exists in the Stern layer as an ion-paired species with LS^-. The environment is a mixture of H_2O and NaLS. Given the propensity for ion-pairing,[19,37] the hydrophobic (aprotic) portion of this mixture is probably the anionic alkyl sulfate group. Solvation at the α-diimine ligand is also consistent with a mixed H_2O–LS^- environment. However, speculation concerning the details of the solvent distribution at this site requires additional data derived from the room temperature emission (vide infra).

Room temperature emission originates from a thermally equilibrated MLCT state, which differs significantly from the ground state. The excited state is best described as a reduced α-diimine ligand radical anion (L^-) bound to a Ru(III) center.[70] This localized excited state has a non-zero dipole moment that results in solvent polarization that is reflected in the room temperature emission parameters. In particular, for the Ru(II) complexes we find $S_M \sim 1$ and $S_L \sim 0$ in the NaLS micelles. The S_L value differs significantly from the aqueous value, and the S_M value is similar to the aqueous value.

We suggest that these changes in S_L may reflect the local solvent environment for the thermally equilibrated MLCT state. Changing the environment from water to an alcohol has the effect of greatly reducing S_L while leaving S_M largely unaffected. The changes in S_L may arise from removal of water from around the excited state and can be used as an indicator of the sensitizer environment in the micelles. The essentially zero S_L on micellization is, thus, consistent with the removal of H_2O from the vicinity of the Ru(III) center.

Clearly then, one of the reasons for increased lifetime and quantum yield on micellization is reduced water exposure of the excited state. Water is a known quencher of MLCT excited states, and reduction of H_2O exposure by micellization reduces the ω_H mode as a means of excited-state deactivation.

One mechanism by which water can be removed from the sensitizer region involves additional ion-pairing in the excited state. In the micelle, the ground-state Ru(II) center ion pairs with the alkyl sulfate groups. Upon formation of the MLCT state, additional sulfate ion pairs form with the newly created Ru(III) center. As tighter ion pairs form, water around the Ru center is extruded. The result is the decrease in S_L with the corresponding increase in the hydrophobicity near the Ru center.

In Table V we compare the spectral fitting parameters for water, micelles, and alcohols for Ru(4,7-Me_2(phen))$_3^{2+}$. Long-chain alcohols have been suggested as reasonable solvent models for spectral structure studies of micelle-bound metal complexes.[37] Our quantitative studies show that alcohols are good micelle models as judged by some spectral parameters but not by others. The S's agree well between the two media, the E^{00}'s are somewhat higher for the alcohols, and the $\nu_{1/2}$'s agree poorly.

In regard to the suggestion that a long-chain alcohol is required for micellar models, we find negligible differences between the spectral parameters for methanol and for decanol. Thus, contrary to earlier beliefs long-chain alcohols are not required to mimic the local environment of micelles. The CH_2OH of the methanol produces most of the observed changes from water. Further, because of the insolubility of these complexes in pure hydrocarbons, the hydroxylic content around the sensitizer must be appreciable.

The results of Table V also support sensitizer binding in the Stern layer. If the complex were bound in a predominantly water environment, S_L in the micelle would approach the value of 2 for pure water, but this is not observed. Conversely, if the binding region were largely hydrocarbon in nature, the longer chain alcohols would be better models and there would be greater differences between the short- and the long-chain alcohols. These results clearly implicate a mixed hydroxyllic–hydrophobic environment around the micellized sensitizer.

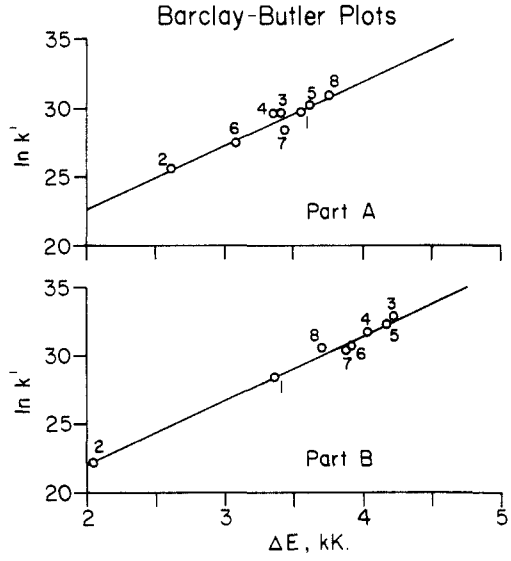

Figure 4. Barclay–Butler plots. Semilogarithmic plots of the preexponential factor, k', vs. the barrier height for the MLCT → d–d transition, ΔE. Part A, water; part B, 50 mM NaLS. The solid lines are the least-squares fits. The complexes are (1) Ru(bpy)$_3^{2+}$; (2) Ru(Me$_2$(bpy))$_3^{2+}$; (3) Ru(phen)$_3^{2+}$; (4) Ru(Cl(phen))$_3^{2+}$; (5) Ru(4,7-Me$_2$(phen))$_3^{2+}$; (6) Ru(4,7-Me$_2$(phen))$_3^{2}$; (7) Ru(5,6-Me$_2$(phen))$_3^{2+}$; (8) Ru(Me$_4$(phen))$_3^{2+}$. Parameters are the following: part A, slope = 4.73 × 10^{-3} cm, intercept = 13.16, correlation coefficient = 0.9535; part B, slope = 4.77 × 10^{-3} cm, intercept = 12.37, correlation coefficient = 0.9910.

Additional evidence supporting our mixed solvation model is available from the study of the MLCT → d–d transition, $d\pi^5$(Ru)π^*(L) → $d\pi^5$(Ru)$d\sigma^*$(Ru). The behavior is summarized by the Barclay–Butler plots[71] for H_2O and 50 mM NaLS micelle solution in Figure 4.[71] While our data do not warrant a quantitative analysis of the solvent effects, two points are worth noting:

(1) The H_2O and micellar plots are strikingly similar. The slopes are identical and equal to that observed for Ru(bpy)$_3^{2+}$ in a series of aprotic organic solvents,[23,25] although the intercepts differ slightly for the different systems.

(2) The linear Barclay–Butler plot for the micellar solution is revealing. For a two-component mixed-solvent system, linear Barclay–Butler plots are observed when (a) the reactant interacts strongly with only one solvent component and (b) the solvents interact negligibly with each other.[72] Thus, the linear plot is consistent with our two-solvent model where we think of the reactant as the MLCT excited state and the micelle represents a two-component solvent system consisting of H_2O and the LS^-. Linearity results since one solvent component is replaced by the other at the sensitizer throughout a series of complexes. Thus, this behavior is identical with that of the solvent exposure parameters and consistent with our earlier arguments (vide supra) regarding solvation of the micellized MLCT state.[73]

We turn now to the intriguing question of the origin of the changes in E^{00}'s with variation in environment and temperature. We examine Ru(4,7-Me_2(phen))$_3^{2+}$ since we have the most data (Table V) on this complex. The major observations are as follows:

(70) Balzani, V.; Bolletta, F.; Gandolfi, M. T.; Maestri, M. *Top. Curr. Chem.* **1978**, *75*, 1.

(71) Barclay, I. M.; Butler, J. A. V. *Trans. Faraday Soc.* **1938**, *34*, 1445.

(72) Leffler, J. E.; Grunwald, E. *Rates and Equilibria of Organic Reactions*; John Wiley: New York, 1963.

(73) It is of interest to note that the specific solvation of transition-metal complexes, especially in mixed solvent systems, by a given solvent proposed here has been noted previously. Specific solvation of Reineckate's salt[74] and our α-diimine Ru(II) sensitizers[75] by MeCN in MeCN/H_2O mixtures has been shown.

(74) Gutierrez, A. R.; Adamson, A. W. *J. Phys. Chem.* **1978**, *82*, 903.

(75) Ayala, N.; Hauenstein, B. L., Jr., work in progress.

(a) E^{00} decreases slightly on going from water to the alcohols at room temperature (250–480 cm^{-1}). (b) E^{00} decreases by 830 cm^{-1} on micellization relative to water at room temperature. (c) E^{00} for the alcohols increases (1020–1170 cm^{-1}) on cooling and glass formation at 77 K. (d) E^{00} for the micellized system increases by 1225 cm^{-1} on freezing to a rigid glass at 77 K. (e) The E^{00}'s for all the 77 K low-temperature media are similar. Thus, there appears to be three distinctly different emission energies depending on media and temperature: a high-energy emission E^{00} associated with all low-temperature media, an intermediate-energy emission associated with room temperature homogeneous media, and a low-energy emission associated with micellization.

We rationalize this behavior by two factors: the reorganizational time scale of the excited state and its environment and the reorganizational energies. First, at low temperature the emission must arise from the initially excited conformation since the excited molecule and its associated environment cannot relax to a thexi state during the excited-state lifetime. The similarity of the E^{00}'s for the alcohols and the micelles at 77 K suggests an initially excited state whose energy is little affected by the environment. This is not surprising given the relative insensitivity of the emission of this class of complexes to different homogeneous environments.

At room temperature the media are quite fluid, relaxation is fast compared to τ, and the emission is exclusively from the thexi state. The differences (>1000 cm^{-1}) between the 77 K and room temperature emissions are largely the energy of stabilization of the thexi state relative to the initially formed excited species.

The appreciably lower E^{00} for the micellar media relative to either water or the long-chain alcohols can be attributed to the greater stabilization of the thexi state. As described above this stabilization arises from the molecular rearrangements of the charged micelle head groups to conform to the newly polarized Ru^{III}–L^- excited state along with the associated conformational changes of the solvent environment.

The sharpening of the emission spectra on cooling is typical of many systems. For the two alcohols and the micelle the $\nu_{1/2}$ decreases by a factor of 2.7 and 2.0, respectively. Assuming that χ_o is temperature independent, eq 9 predicts a factor of 2.0. Thus, eq 6–9 appears to account in large measure for the observed spectral narrowing on cooling.

The apparent narrowing of the emission spectra on micellization at room temperature is not predominantly due to a decrease in the $\nu_{1/2}$'s. While there is a small decrease, the effect is not large enough to account for the pronounced spectral sharpening. The major factor appears to be loss of the low frequency metal vibrational mode, ω_L, as reflected by the reduction in S_L on micellization. The superposition of the low-frequency vibration in water has the effect of blurring the vibrational structure of the dominant high-frequency mode, and thus broadening the spectra.

Conclusion

Our results provide a considerable insight into the energy degradation pathways and structure of micellized sensitizers.

(1) The temperature dependencies of the sensitizer τ's in H_2O and in NaLS micellar solution aid in determining energy degradation pathways. Our data indicate that the increased τ's and luminescence yields on micellization arise in large part from stabilization of the emitting MLCT state relative to the d–d state; the resultant higher barrier to degradation via the MLCT → d–d transitions reduces this rate. Further, since photodecomposition of Ru(II) sensitizers in large measure proceeds via the photoactive d–d state,[25,44-48] micellization should increase sensitizer photostability by decreasing the efficiency of d–d state population. This observation is of special importance given the interest in micelle-based solar energy conversion schemes.[3,7-9]

(2) Another important cause of the increased τ's on micellization is the decrease in k_{nr}. Qualitatively, nonradiative decay theory indicates that the decrease in k_{nr} is due primarily to a decrease in S_L upon micellization. The k_{nr}'s obtained from the temperature dependence of τ appear to deviate more from the values calculated from the emission spectra and decay theory as the sensitizer hydrophobicity increases. We can ascribe this disagreement to the exclusion of contributions to k_{nr} from high-frequency hydrogen-bonding solvent-acceptor modes.

(3) Quenching behavior and sensitizer solvent exposure is most consistent with binding in the Stern layer at the micelle surface. The parameters characterizing the emission spectra in the micelle solution provide insight into the bound sensitizer's environment. In the ground state, there is extensive ion-pairing of Ru(II) with LS^-. Water is present at the Ru(II) center and the α-diimine ring. The MLCT excited state experiences a decreased H_2O content at the Ru center.

(4) Except for $Ru(bpy)_3^{2+}$, all sensitizers exhibit similar spectral emission behavior upon micellization. $Ru(bpy)_3^{2+}$ is also somewhat anomalous in quenching behavior, where we have attributed the differences to the smaller size and larger electrostatic interaction of the complex with its environment.[76] The increased $\nu_{1/2}$ ($\propto \chi_o$) for $Ru(bpy)_3^{2+}$ also suggests a tighter, more intimate ion-pair for this complex. The differences are not really surprising since the larger charge/radius ratio for $Ru(bpy)_3^{2+}$ compared to the remaining sensitizers yields increased reorganizational energy and decreased quenching rates.

(5) The changes in excited-state energies with solvent and temperature can be rationalized on the basis of relaxational energies and times on going from the initially excited species to the (thexi) state.

It is clear that the homogeneous model can be successfully adapted to micellar media. We are currently exploring the utility of these models in other organized media.

Acknowledgment. We gratefully acknowledge support by the donors of the Petroleum Research Fund, administered by the American Chemical Society, and the National Science Foundation (CHE 82-06279 and 86-00012). All lifetime measurements were carried out on the University of Virginia laser facility purchased in part through National Science Foundation Grant CHE 77-09296.

Registry No. NaLS, 151-21-3; $Ru(bpy)_3^{2+}$, 15158-62-0; $Ru(Me_2(bpy))_3^{2+}$, 32881-03-1; $Ru(phen)_3^{2+}$, 22873-66-1; $Ru(Cl(phen))_3^{2+}$, 47860-47-9; $Ru(Me(phen))_3^{2+}$, 14975-39-4; $Ru(4,7\text{-}Me_2(phen))_3^{2+}$, 24414-00-4; $Ru(5,6\text{-}Me_2(phen))_3^{2+}$, 14975-40-7; $Ru(Me_4(phen))_3^{2+}$, 64894-64-0; H_2O, 7732-18-5; methyl alcohol, 67-56-1; ethyl alcohol, 64-17-5; *n*-butyl alcohol, 71-36-3; *n*-hexyl alcohol, 111-27-3; *n*-octyl alcohol, 111-87-5; *n*-decyl alcohol, 112-30-1.

(76) Hauenstein, B. L., Jr.; Dressick, W. J.; Demas, J. N.; DeGraff, B. A. *J. Phys. Chem.* **1984**, *88*, 2418.